



## Characterisation and calibration of active sampling Solid Phase Microextraction applied to sensitive determination of gaseous carbonyls

Elena Gómez Alvarez<sup>a,b,\*</sup>, Mónica Vázquez Moreno<sup>b</sup>, Sasho Gligorovski<sup>a,\*</sup>, Henri Wortham<sup>a</sup>, Miguel Valcárcel Cases<sup>c</sup>

<sup>a</sup> Université d'Aix-Marseille I, II, III-CNRS, UMR 6264: Laboratoire Chimie Provence, Equipe Instrumentation et Réactivité Atmosphérique, Case courrier 29, 3 place Victor Hugo, F-13331 Marseille Cedex 3, France

<sup>b</sup> Fundación Centro de Estudios Ambientales del Mediterráneo (CEAM), C/Charles Darwin, 14 Parque Tecnológico, 46980 Paterna, Valencia, Spain

<sup>c</sup> Dpto de Química Analítica, Edificio Marie Curie (Anexo), Campus Universitario de Rabanales, 14071 Córdoba, Spain

### ARTICLE INFO

#### Article history:

Received 29 June 2011

Received in revised form 9 October 2011

Accepted 16 October 2011

Available online 31 October 2011

#### Keywords:

Automation

Field sampling of gaseous carbonylic compounds

PFBHA on-fibre derivatisation SPME

### ABSTRACT

A characterisation of a system designed for active sampling of gaseous compounds with Solid Phase Microextraction (SPME) fibres is described. This form of sampling is useful to automate sampling while considerably reducing the sampling times. However, the efficiency of this form of sampling is also prone to be affected by certain undesirable effects such as fibre saturation, competition or displacement effects between analytes, to which particular attention should be paid especially at high flow rates. Yet, the effect of different parameters on the quantity of the results has not been evaluated. For this reason, in this study a careful characterisation of the influence of the parameters involved in active sampling SPME has been performed. A versatile experimental set-up has been designed to test the influence of air velocities and fluid regime on the quantity and reproducibility of the results. The mathematical model applied to the calculation of physical parameters at the sampling points takes into consideration the inherent characteristics of gases, distinctive from liquids and makes use of easily determined experimental variables as initial/boundary conditions to get the model started.

The studies were carried out in the high-volume outdoor environmental chambers, EUPHORE. The sample subjected to study was a mixture of three aldehydes: pentanal, hexanal and heptanal and the determination methodology was O-(2,3,4,5,6-pentafluorobenzyl)-hydroxylamine hydrochloride (PFBHA) on-fibre derivatisation.

The present work proves that the determination procedure is quantitative and sensitive, independent from experimental conditions: temperature, relative humidity or ozone levels.

With our methodology, the influence on adsorption of three inter-related variables, i.e., air velocity, flow rate and Reynolds numbers can be separated, since a change can be exerted in one of them while keeping the others constant.

© 2011 Elsevier B.V. All rights reserved.

### 1. Introduction

Some of the calibration procedures using adsorptive SPME reported in the literature are based on theoretical principles (e.g., heat-mass transfer). Their practical application presents a certain degree of difficulty. These quantification approaches have been summarised in the review by Ouyang and Pawliszyn [1]. Of special relevance are two diffusion-based calibration procedures applied

to air in convection conditions: the interface model developed by Koziel et al. [2] and the cross-flow model by Chen et al. [3]. The main difficulty of these methodologies is that they require the experimental determination of air velocity at the sampling point.

Due to these difficulties of quantification with adsorptive SPME and the occurrence of unwanted effects (fibre saturation, displacement or competition between analytes) which can hinder accurate/quantitative determinations, a number of analysts have opted for non-equilibrium quantification [4–10].

The interface model developed by Koziel et al. [2] describes quantification according to the following equation:

$$n = \left( \frac{DA}{\partial} \right) C \cdot t \quad (1)$$

which is valid for the special case that is the thickness of the boundary layer is much smaller than the outer radius of the fibre. This

\* Corresponding authors at: Université d'Aix-Marseille I, II, III-CNRS UMR 6264: Laboratoire Chimie Provence, Equipe Instrumentation et Réactivité Atmosphérique, Case courrier 29, 3 place Victor Hugo, F-13331 Marseille Cedex 3, France.

Tel.: +33 4 13 55 10 48/+33 4 13 55 10 52; fax: +33 4 13 55 10 60.

E-mail addresses: [elenaceam@hotmail.com](mailto:elenaceam@hotmail.com) (E. Gómez Alvarez), [saso.gligorovski@univ-provence.fr](mailto:saso.gligorovski@univ-provence.fr) (S. Gligorovski).

equation has been adapted from Fick's law of diffusion, where the area of the circle is replaced by  $A$ , surface area of the sorbent (in SPME the whole cylinder is exposed to the gaseous sample), and  $Z$  is replaced by  $\delta$ , thickness of the boundary layer.

The effective thickness of the boundary layer can be described as the location where the transition occurs between the analyte flux in the bulk sample being controlled by diffusion to being controlled by convection. Experimental research has indicated that convection plays also a role inside the boundary layer. However, its effect decreased with the distance to the solid surface [11].

In order to apply Fick's law of diffusion, the concentration of the air exiting the adsorbent material should be taken into consideration, except for very efficient adsorbents in which the air after crossing the fibre is completely depleted of the analyte. This requirement is replaced by the assumption that the fibre behaves as zero sink, i.e., in the proximity of the fibre, the concentration of analyte is close to zero, which is the case for very efficient adsorbents.

If the air velocity is well over the critical air velocity of  $10 \text{ cm s}^{-1}$ , the estimation of the boundary layer thickness is the same as for the critical velocity. The basis of this approach was that devices that allow extractions using air speeds higher than the critical limit, would ensure better analytical precision and accuracy, since variations in air velocity would not affect the mass uptake rate.

In this work we pursue a number of objectives. On the one hand, we intend to calibrate the methodology of sampling with adsorptive SPME fibres based on parameters that can be readily experimentally measured, avoiding in this way theoretical assumptions. On the other hand, we want to develop an experimental set-up that enables us to automate the methodology and is at the same time versatile. With this, we aim at evaluating the contribution of the different parameters independently and their effect on the quantity and reproducibility of the methodology. The developed methodology has been tested in the EUPHORE chamber facility.

## 2. Experimental

### 2.1. Description of the EUPHORE facilities

The facility consists of two identical half sphere chambers made of Teflon foil, each with a volume of approximately  $200 \text{ m}^3$ . The chambers are equipped with conventional analytical instrumentation and some apparatus specific to the determination of certain parameters relevant in atmospheric chemistry studies. The absolute humidity of the air inside the chambers is monitored by a dew point mirror measuring system.

The chambers are sheltered from the atmospheric influences by two half-sphere-shaped protective houses. The air used in the experiments is supplied by gas purification units.

Integrated into the flanges are ports for the input of reactants and sampling lines for the different analytical instruments. In order to ensure rapid homogenisation in the chamber, two mixing fans with an air throughput of  $4000 \text{ m}^3 \text{ h}^{-1}$  each are installed in the chamber. 5 ml of  $\text{SF}_6$ -the dilution tracer-is introduced into the chamber through one of the ports in a chamber flange. It can be monitored during the course of the reaction by FTIR.

### 2.2. Chemicals and materials

The following chemicals were used: O-(2,3,4,5,6-pentafluorobenzyl)-hydroxylamine hydrochloride (PFBHA), puriss. p.a. >99.0% (HPLC), MW: 249.57 (Fluka Chemie GmbH,

Switzerland).  $65 \mu\text{m}$  PDMS/DVB SPME fibres (Supelco, USA). Valeraldehyde (pentanal) – Aldrich, capronaldehyde (hexanal) – Fluka and heptanal – Fluka were also used for the experiments.

Stainless steel nuts and Teflon ferrules were supplied by Swagelok (Válvulas y Conexiones Iberica, S.L., Barcelona, Spain). 4.34, 8 and 16 mm i.d. tubing were supplied by Technyfluor, Terrasa (Barcelona, Spain).

### 2.3. Instrumentation and methods for SPME determinations in gas phase

#### 2.3.1. Chromatographic conditions

A 6890 HP Gas Chromatograph with a flame ionization detector (FID) was used which was equipped with a HP-5 MS crosslinked 5% PHME siloxane  $30 \text{ m} \times 0.250 \text{ mm} \times 0.25 \text{ mm}$  capillary column and an inlet liner of internal diameter of 0.75 mm i.d. Pre-drilled Thermogreen LB-2 septa for SPME.

**GC conditions:** The Gas Chromatograph was programmed at  $80^\circ\text{C}$  for 2 min, then ramped at a rate of  $20^\circ\text{C}/\text{min}$  to  $280^\circ\text{C}$  and held for 3 min. Total chromatography time was 15 min. The injection port was held at  $270^\circ\text{C}$  and the detector was held at  $300^\circ\text{C}$ .

#### 2.3.2. PFBHA on-fibre derivatisation SPME. Sampling description

Previous to their initial use, the fibres were conditioned by inserting them in the injector of the Gas Chromatograph at  $250^\circ\text{C}$  for half an hour according to manufacturer's instructions.

The derivatising reagent was loaded on the  $65\text{-}\mu\text{m}$  thick PDMS/DVB fibre. Loading was performed from the headspace of a 4 ml opaque amber vial containing a well-agitated  $17 \text{ mg ml}^{-1}$  O-(2,3,4,5,6-pentafluorobenzyl)-hydroxylamine hydrochloride derivatising solution. This solution was prepared daily and during the experiments, maintained at room temperature. The septum was punctured with the fibre sheath to a depth of 0.5 cm, as the loading of the derivatising agent is performed from the headspace. After 2 min, the fibre was retracted and removed from the vial. The needle was again adjusted to full length, and sampling was performed for varying times according to the observed sensitivity and flow rates attained by the different set-ups.

#### 2.3.3. Additional instrumentation used in the experiments

The following analytical instrumentation was also used for the time-resolved determination of the aldehydes introduced in the chamber and monitoring of dilution: a GC Fisons 8160 (San Jose, CA, USA) with photo-ionization (PID) and flame ionization detection (FID) and FTIR spectroscopy.

Air samples are collected automatically in a sampling loop and then injected into the chromatograph. The Fisons GC-8160 is equipped with a 30 m DB-624 (cyanopropylphenyl polysiloxane) fused silica capillary column (J&W Scientific, 0.32 mm id,  $1.8 \mu\text{m}$  film). Due to changes in the PID baseline the chromatograph is usually operated at isothermal conditions ( $80^\circ\text{C}$ ). The rest of the chromatographic conditions were: column DB-624, 30 m, i.d.: 0.32 mm  $1.8 \mu\text{m}$ , injector temperature  $80^\circ\text{C}$ . Detectors temperature:  $250^\circ\text{C}$ ,  $P_{\text{He}}$  25 kPa,  $P_{\text{H}_2}$  70 kPa,  $P_{\text{air}}$  100 kPa,  $P_{\text{N}_2}$  (PID Purge) 20 kPa, PID lamp 10.6 eV, column flow 1.6 ml/min (120 kPa), split 1/75, splitless from 1 to 4 s (time of injection). The sample acquisition rate is set to 10 min.

A FTIR spectrometer (NICOLET, MAGNA 550, resolution of  $1 \text{ cm}^{-1}$ , MCT/A detector) with a KBr beamsplitter is used to determine at any time the concentration of precursors and products during the course of the reaction. It is used for trace gas detection in the infrared spectral range between 400 and  $4000 \text{ cm}^{-1}$ , in combination with a long-path absorption system. Liquid  $\text{N}_2$  (Praxair) was used to cool down the detector. The dilution was measured

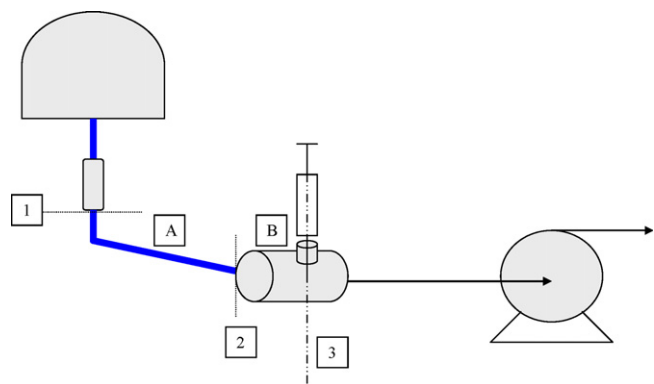


**Fig. 1.** Experimental set-up for active sampling SPME in which 1, is the location of the flow meter where a precise measurement of flow rate, pressure and temperature is provided, and therefore can be taken as initial point for the calculations; B, denotes the enlargement zone that hosts the SPME holder; 2, is the entrance to the flow-through cell; 3, is the section of flow-cell where sampling takes place.

following the decay of  $SF_6$ , an initially added inert tracer, by means of FTIR. The sample acquisition rate is set to 10 min.

#### 2.4. Experimental set-up

The experimental set-up in which the system for active sampling was implemented is displayed in Fig. 1. SPME sampling from the chamber was performed by using a system of active sampling. The sampling cell is especially designed to allow insertion of the SPME fibre. The internal design of the sampling cell and of the rest of the components of the active sampling system, were characterised applying principles of fluid dynamics to allow the evaluation of the impact of certain variables on the sampling efficiency. The parameters subjected to evaluation were fluid regime, air velocity and total mass of compounds to which the fibre is exposed (all directly related to flow rate). In the following section, a detailed description of the sampling cell designs subjected to study is provided.

In order to introduce changes in these parameters, it is necessary to vary the flow rate (total flow). A critical orifice was installed in the adaptor that connects the system to the chamber. In addition, it is also possible to vary the system tubing diameters (doing this has the same effect as installing critical orifices), the internal diameter of the sampling cell and the overall capacity of the pump. A KNF Neuberger GmbH N0150AN.9E gas diaphragm pump (Freiburg, Germany) was used.

A TSI Inc. Series 4000/4100 (Shoreview, MN, USA) mass flow meter was connected inline—using home-made Teflon adapters which enabled screwing on the Teflon tubing and provided pressure, temperature and exact flow during sampling with an acquisition frequency of  $0.5\text{ s}^{-1}$ . The mass flow meter was periodically calibrated providing a precision of 0.27% (calculated as 3 times the standard deviation of the calibration slope).

This experimental set-up allows introducing changes in certain system parameters, such as total flow and air velocity at the sampling point, by varying the internal diameters of the different components relative to each other, such as the tubing located just before the sampling cell entrance and the internal diameter of the sampling cell itself.

##### 2.4.1. Design of active sampling flow cells

As stated previously, the experimental set-ups are designed with the aim to obtain versatility in the experimental conditions, in order to evaluate the effect of the different parameters on the sampling efficiency. In the first stage of the development, two different designs of flow cells (made of Teflon) were essayed, i.e., in one the

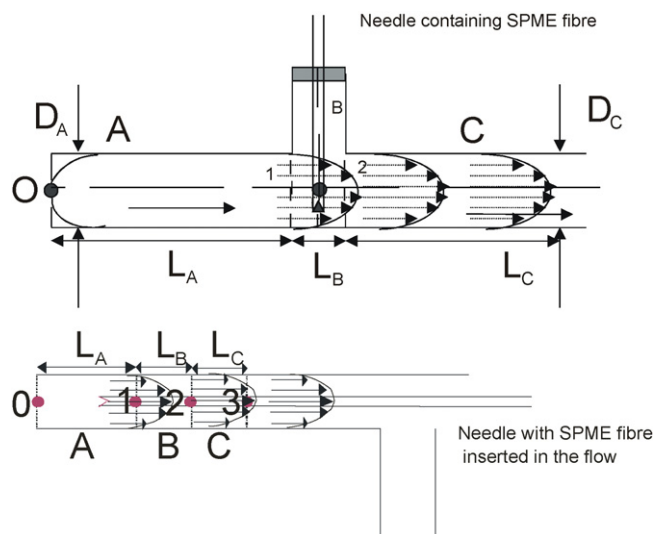


**Fig. 2.** Designs of flow-through cells that hosts SPME fibre. (A) Sampling cell in which sampling takes place perpendicularly to the flow direction. (B) Sampling cell in which sampling takes place parallel to the flow direction.

fibre was located perpendicular to the direction of the flow and in the other, the fibre laid parallel to the flow (Fig. 2). Fig. 2A and B shows the advance of the flow and the SPME needle sampling from the cell in both cell designs.

Follows the description of the flow-through cell that hosts the SPME fibre in the set-up for active sampling.

Fig. 2 is a planar representation of the cell design. The following points are marked along an imaginary line drawn parallel to the flow.  $O$  represents a point at the entrance of the flow-through cell,  $L_A$  is the length of the tube prior to the enlargement designed to allow insertion of the fibre holder and needle,  $L_B$  is the length at enlargement, and  $L_C$ , the length after enlargement.  $D_A$ ,  $D_B$  and  $D_C$  are the respective diameters at these three sections. The inner diameter of the tube extension that hosts the holder adapter was set at 0.004 m. Due to its small diameter, this section acts as a guide for the introduction of the SPME needle. The length of the tube at its extension was set at 0.035 m to host the holder and, considering the needle length, to ensure that the fibre was centred in the flow of air ( $D_B$  – diameter of sample tube at B – is calculated as  $D_A + 0.035$  m.  $D_C$  and  $D_A$  are equal).

The minimum inner diameter of the flow-through tube had to be over the fibre length estimated at  $1.02 \pm 0.03$  cm in a study (12) in which a comparison of PDMS (100  $\mu\text{m}$ ) fibre lengths ( $n = 13$ ) was made. It is advisable to make  $D_A$  a few millimetres larger, to prevent damage to the fibre by collision with the walls.

The second cell configuration was designed in such a way that the fibre lays parallel to the direction of the flow during sampling. The equations applied to the calculations were exactly the same as in the other design. The only difference lies on the configuration and the way sampling takes place. In the case of the parallel design, the calculations are considerably simpler since there is no enlargement introducing an alteration in the sample flow. The performance of this system in terms of air velocities achievable at varying flow rates was quite good. A diameter of 4 mm was essayed in correlation with the diameter in the sampling area ( $D_B$ ) chosen in the previous design. The increase in  $D$  had as consequence a noticeable drop in air velocities for comparable flow rates. However, the increase in length in section A ( $L_A$ ) had a negligible effect on air velocities. Unlike the previous design, there were no remarkable differences between the parameters observed in sections B and C on behalf of section A.

## 2.5. Characterisation of active sampling system

To adequately characterise the circulation of fluids in a pipe, theoretical principles of fluid dynamics were applied. All processes contributing to the irreversible transformation of mechanical energy into internal energy/heat need to be considered, e.g., pressure, difference in height between two points, velocity and density in each section of the conduction, loss of mechanical energy or energy supplied by an external device.

The densities of gases vary differently with pressure. Consequently, the equations applied to describe them will be different too. In the case of gases, density is almost directly proportional to pressure and also depends strongly on temperature. The Supporting Information presents the model including the calculations applied for the characterisation of the systems with parallel or perpendicular cells applying basic principles of fluid dynamics [12–17].

## 3. Results and discussion

### 3.1. Inter-day and inter-fibre reproducibility

Reproducibility tests were carried out at 245 litres per minute (lpm) (only attainable with the set-up of 16 mm i.d.) on the same day, by taking 6 samples after the insertion of 100  $\mu\text{l}$  of each analyte into the chamber. Sampling steps were carried out alternatively with two different fibres (65  $\mu\text{m}$  PDMS/DVB). Sampling times were 10 and 30 s.

To evaluate system reproducibility, SPME responses were plotted versus total mass of compound crossing the fibre. The estimated variability could be considered an intra-day, inter-fibre estimation of reproducibility in a wide range of total mass crossing the fibre. An overall reproducibility of 4.4% was estimated.

### 3.2. Evaluation of experimental parameters on sampling

The effect of temperatures in the 10–50  $^{\circ}\text{C}$  range was essayed applying stepwise increases of 5 or 10  $^{\circ}\text{C}$ , finding no remarkable influence of the temperature on the results obtained.

We know that humidity and ozone levels do not affect the results obtained since the methodology developed at EUPHORE and here presented was tested in a formal Intercomparison campaign [19].

The dependence of temperature was tested at the following temperatures: 10, 20, 30, 35, 40, 45, and 50  $^{\circ}\text{C}$ . The figures representing the variations with temperature can be found in S.I. The RSD (%) between the results obtained at different temperatures was lower than 10.2% for pentanal, 6.6% for hexanal and 6.4% for heptanal.

### 3.3. Tests on different tests designs

Although the effect of air velocity on the uptake efficiency of analytes in adsorptive sampling SPME has been investigated [2,3,5,8] there are still issues that remain not completely understood. It seems accepted that dynamic conditions (movement of air) have a positive effect on the adsorption of analytes [2]. It would therefore be useful to obtain complementary information about the effect of applying high sampling flow rates exceeding the critical values in the range of a few  $\text{m s}^{-1}$ . In addition, it would be interesting to know if it is just the flow rate that has an effect on adsorption or the air velocity, too. Finally, we wanted to understand the consequences of sampling in laminar or turbulent conditions. These questions arose after the observation that in situ sampling in the EUPHORE chambers, where the air velocity is estimated to be  $4 \text{ m s}^{-1}$ , achieved better sensitivity than active sampling at rates that caused the air to flow at lower velocities.

**Table 1**

Air velocity and Reynolds numbers associated with a number of active sampling conditions applied using the parallel cell design.

FC setting (%) <sup>a</sup>	Q (lpm)	Reynolds number (Re)	$v_1^b$ ( $\text{m s}^{-1}$ )	Regime
10	1.73	395	1.02	Laminar
19	3.17	723	1.87	Laminar
28	4.61	1052	2.72	Laminar
40	6.53	1490	3.85	Laminar
50	8.12	1854	4.79	Laminar
60	9.72	2220	5.73	Transition
70	11.32	2584	6.67	Transition
80	12.92	2950	7.62	Transition

<sup>a</sup> Flow controller setting in percentage.

<sup>b</sup>  $v_1$  denotes the air velocity at the point of sampling in the parallel cell design.

As it was possible to obtain different values of air velocity at the sampling point using the different cell designs within the working intervals of sampling flow rates, this fact was taken to advantage to essay the potential effect of air velocity on the efficiency (in order to study if the sensitivity could be improved by increasing the air velocity at the sampling point).

Fig. 3A shows a graphical representation of fibre responses versus flow rate for the parallel and perpendicular cell designs. In all cases a variation of the response with the flow for each one of the designs has been observed (although eventually showing certain signs of saturation).

In Fig. 3B a plot of fibre responses versus air velocity is displayed. In this graphical representation, a distinctive behaviour can be observed of each one of these designs. The perpendicular design shows a better sampling efficiency. In Fig. 3B, a clear influence of velocity on the sampling efficiency can be observed in either one of these designs. However, the fact that the increase in efficiency does not depend exclusively on air velocity, points at an important but not determinant effect of the latter, and in consequence that calibration could not be performed exclusively in terms of air velocity.

Additionally, the influence of fluid regime (laminar, transition or turbulent) was tested for their expected influence on the reproducibility of the results. Table 1 displays the values of air velocity and Reynolds numbers associated with a number of active sampling conditions applied using the parallel cell design.

It can be observed that with this design wider interval in terms of air velocity could be attained as compared with the perpendicular flow-through cell design (Table 2). Even differences in the maximum flow rates (lpm) attainable could be observed, which shows the impact of the design of the sampling system on the resulting experimental parameters.

In Table 2 only three of the settings shown in Table 1 were selected for the parallel cell design and compared with three settings of flow rate applied in the perpendicular cell. It can be observed that for the parallel cell different situations were essayed in terms of fluid regime, which does not seem to be determinant either in the quantity of the results. The parameters represented in Tables 1 and 2 correspond to the points represented in Fig. 3.

### 3.4. Quantitation based on total mass that crosses the fibre

As a form of calibration, the representation of fibre response versus the total mass crossing the fibre during sampling is plotted in Fig. 4A–C for pentanal, heptanal and hexanal, respectively.

In order to calculate the total mass the fibre was exposed to in the course of the sampling, the concentration values provided by the GC-PID during the experiments in ppbV were transformed into  $\mu\text{g m}^{-3}$  by applying the simple calculation presented in the following equation (Eq. 2) [18]:

$$c \text{ (}\mu\text{g m}^{-3}\text{)} = \text{mixing ratio (ppbV)} \times \text{MW molecular} \times 0.409 \quad (2)$$

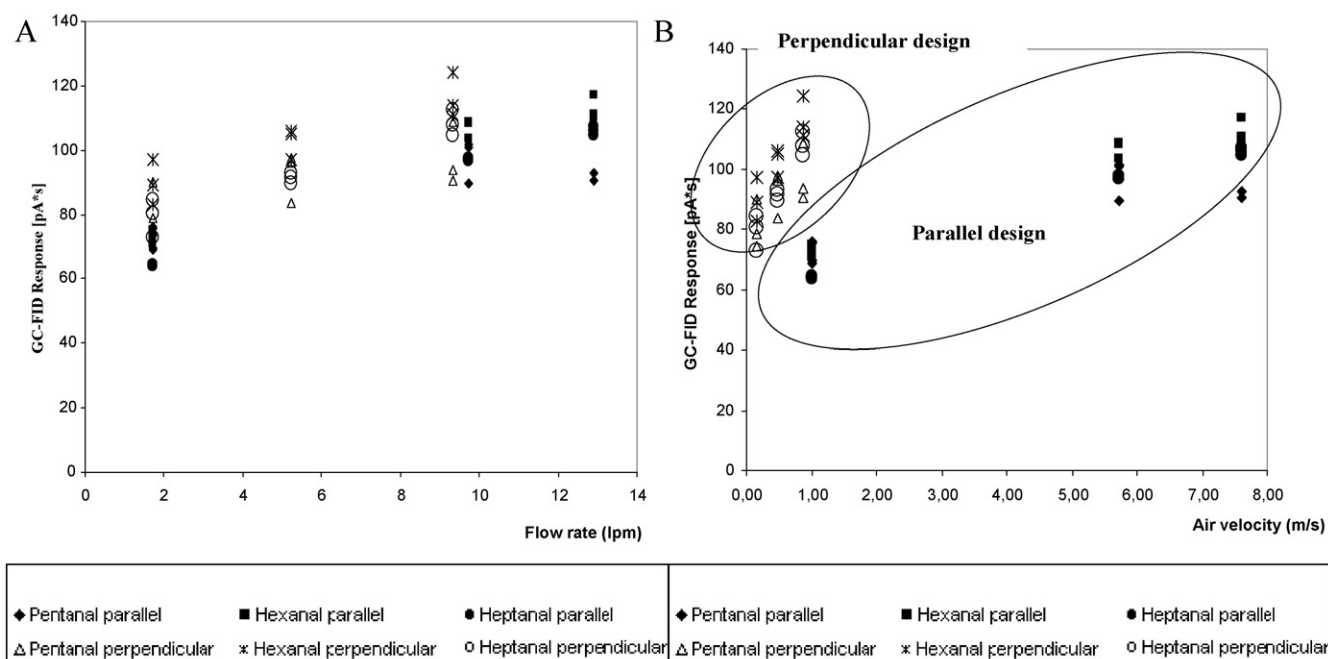


**Fig. 3.** (A) Combined graphical representation of fibre responses versus flow rate for both flow-cell designs. (B) Combined graphical representation of fibre responses versus air velocity for both flow-cell designs.

**Table 2**

Reynolds number and regimes associated at each one of the experimental conditions applied to the study of fibre responses with variations in the velocity of air.

Cell configuration	FC setting <sup>a</sup> (%)	Q (lpm)	$v_1^b$ (m s <sup>-1</sup> )	Reynolds number	Regime
Parallel	10	1.73	1.02	395	Laminar
Parallel	60	9.72	5.73	2220	Early transition
Parallel	80	12.92	7.62	2950	Transition
Perpendicular	10	1.62	0.16	157	Laminar
Perpendicular	33	5.21	0.49	477	Laminar
Perpendicular	60	9.32	0.88	851	Laminar

<sup>a</sup> Flow controller setting in percentage.

which can be further transformed in total mass in  $\mu\text{g}$  by taking into account the average flow rate together with the sampling time. In Eq. 2,  $c$  represents the concentration and MW, molecular weight of the analyte to be determined.

The analytical parameters associated to the calibration together with the experimental parameters at the sampling point are presented in Table 3. The conditions under which the different calibrations were carried out are provided together with the regression

coefficients and the precision of the calibration as precision of the slope. These calibrations represent the individual curves that were used to produce Fig. 4 which represents the assembly of all calibrations together (the individual calibrations were built as SPME response versus the product concentration in the gas phase-sampling time, while the plots presented in Fig. 4 have total mass of analyte as abscises). Both plots are equivalent since they represent a measure of the mass of analyte that crosses the fibre. Table 3,

**Table 3**

Analytical parameters of the calibrations and experimental parameters associated at the point of sampling.

Description of calibration set-up	Flow rate (lpm)	Air velocity (m s <sup>-1</sup> )	Reynolds number	Flow regime <sup>a</sup>	Slope	$r^b$	LOD <sup>c</sup> (ppbV)	Sampling time (min)
<b>Pentanal</b>								
8 mm i.d. tubing, 11 and 15 mm i.d. cell	125	1.34/1.08	3722/3284	Tr/Tr	$2.57 \pm 0.03^b$	0.99	1.10	1.0
16 mm i.d. tubing, 16 mm i.d. cell	245	2.05	6539	T	$6.2 \pm 0.3$	0.97	2.61	0.2
<b>Hexanal</b>								
4.3 mm i.d. tubing, 15 mm i.d. cell	1.6	0.014	44	L	$1.94 \pm 0.03$	0.99	0.19	2.0
4.3 mm i.d. tubing, 15 mm i.d. cell	7.5	0.065	206	L	$2.71 \pm 0.07$	0.99	0.14	2.0
8 mm i.d. tubing, 11 and 15 mm i.d. cell	125	1.34 <sup>d</sup> /1.08	3722/3284	Tr/Tr	$4.57 \pm 0.08$	0.99	0.16	1.0
16 mm i.d. tubing, 16 mm i.d. cell	245	2.05	6539	L	$9.0 \pm 0.3$	0.98	0.49	0.2
<b>Heptanal</b>								
8 mm i.d. tubing, 11 and 15 mm i.d. cell	125	1.34/1.08	3722/3284	Tr/Tr	$4.4 \pm 0.1$	0.99	0.06	1.0
16 mm i.d. tubing, 16 mm i.d. cell	245	2.05	6539	L	$10.8 \pm 0.4$	0.99	0.14	0.2

<sup>a</sup> Flow regime: turbulent (T),  $Re > 4000$ ; transition (Tr),  $4000 < Re < 2100$ ; laminar (L),  $Re < 2100$ .

<sup>b</sup> Precision of the slope.

<sup>c</sup> Backgrounds were estimated as the average plus three times the standard deviation of the blank value ( $n = 5$ ), i.e., sampling performed from the clean chamber before the introduction of the analytes.

<sup>d</sup> The value of  $1.34 \text{ m s}^{-1}$  corresponds to the 8 mm i.d. tubing and 11 mm i.d. cell, while  $1.08 \text{ m s}^{-1}$  corresponds to the 8 mm i.d. tubing and 15 mm i.d. cell set-up.

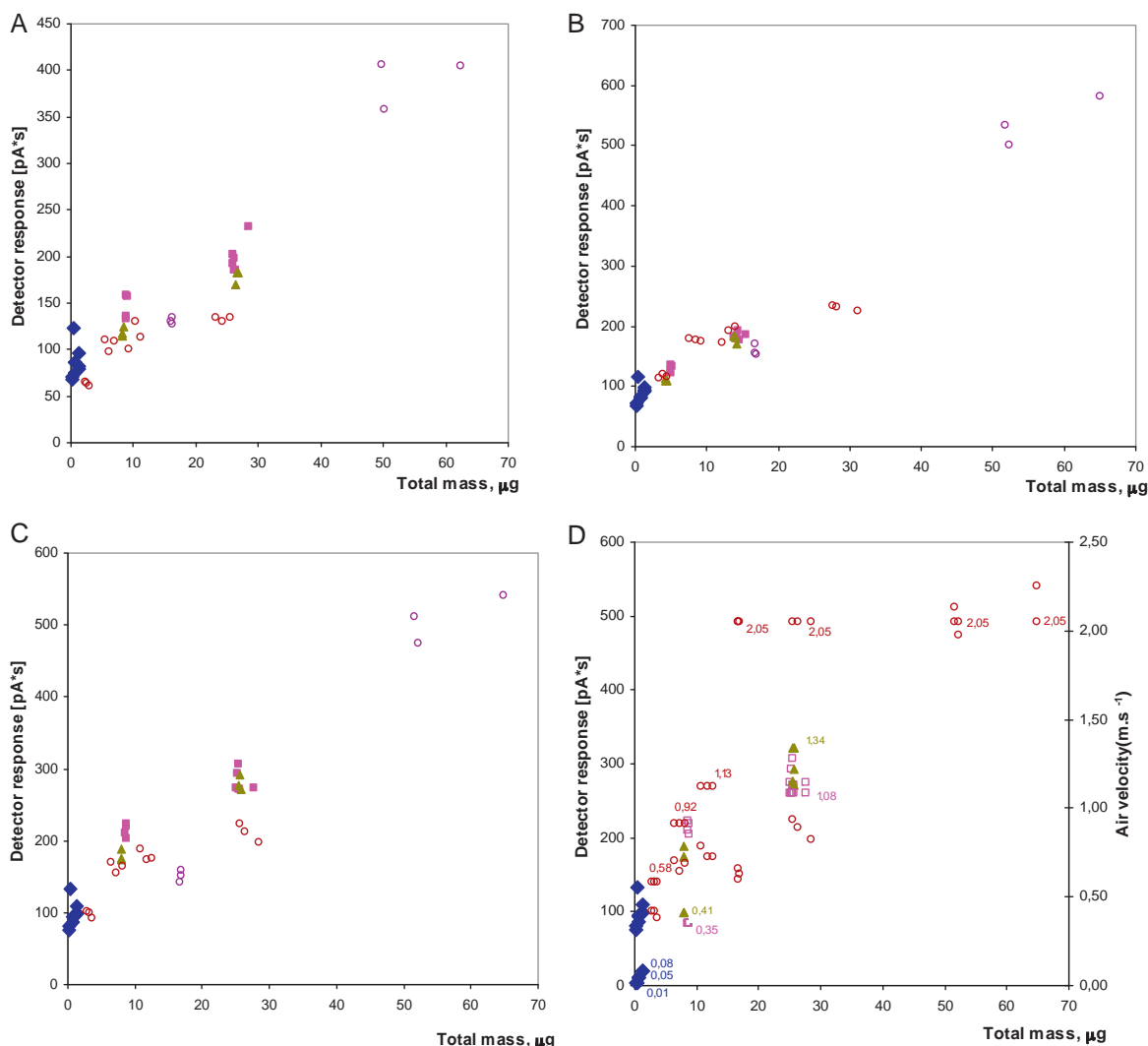


**Fig. 4.** Calibration for pentanal, hexanal and heptanal on behalf of total mass the fibre is exposed to. The different calibration points were typically obtained after introducing the same amount of the three aldehydes pentanal, hexanal and heptanal into the chamber and varying the flow setting during the sampling. (A) Calibration for pentanal; (B) calibration for heptanal; (C) calibration for hexanal; (D) same graph as 4 C for hexanal including air velocities. *Filled diamonds* correspond to set-up with tubing of 6.35 mm, 15 mm i.d. cell. The flows measured were  $1.6 \pm 0.03$ ,  $5.21 \pm 0.09$  and  $9.31 \pm 0.16$  lpm, corresponding Reynolds numbers 44 (laminar flow), 143 (laminar flow) and 256 (laminar flow) respectively; air velocities 1.4, 4.5 and  $8.1 \text{ cm s}^{-1}$ . *Filled squares* correspond to set-up of 8 mm i.d. and 15 mm i.d. cell; flow rates 40 and 120 lpm; Reynolds numbers of 1100 (laminar flow) and 3285 (transitional flow), air velocities of  $34.8 \text{ cm s}^{-1}$  and  $1.1 \text{ m s}^{-1}$ . *Filled triangles* set-up of 8 mm tubing, 11 mm i.d. cell; flow rates of 40 and 125 lpm; Reynolds numbers 1197 (laminar flow) and 3722 (transitional regime) and air velocities of  $412 \text{ cm s}^{-1}$  and  $1.5 \text{ m s}^{-1}$ . *Empty circles* set-up composed by 16 mm i.d. tubing and 16 mm i.d. cell; flow rates 70, 110, 135 and 245 lpm; Reynolds numbers 1407 (laminar), 2797 (transitional), 3535 (transitional) and 6539 (turbulent) respectively, and air velocities were  $58 \text{ cm s}^{-1}$ ,  $92 \text{ cm s}^{-1}$ ,  $1.1$  and  $2.0 \text{ m s}^{-1}$ .

The common graphs presented in Fig. 4 provided the following equations: pentanal  $(5.1 \pm 0.3)x + (68.55 \pm 6.32)$ ;  $r^2 = 0.87$ ; hexanal  $(6.8 \pm 0.4)x + (97.7 \pm 8.0)$ ;  $r^2 = 0.89$ ; heptanal  $(7.4 \pm 0.3)x + (79.4 \pm 5.8)$ ;  $r^2 = 0.93$ .

also displays the LOD obtained in each one of the curves, thereby proving the good sensitivity attainable with these systems of active sampling.

Fig. 4 integrates all the results obtained with the different systems subjected to study and represents SPME response obtained versus total mass in micrograms ( $\mu\text{g}$ ) that crosses the fibre. This parameter accounts for differences in sampling rates, sampling times and dilution, and therefore is a suitable way to normalise the fibre response. The graphs represent eight different series corresponding to calibrations carried out with eight different set-ups.

Fig. 4A–C shows the relationship between SPME responses (as detector response) with the total mass the fibre is exposed to. Fig. 4D corresponding to hexanal, shows simultaneously the velocities of the air circulating through the system for each of the samplings. The exact same values of air velocities apply to the

sampling points of pentanal and heptanal since sampling of the three carbonyls occur simultaneously in the same sampling step. It can be seen that air velocities are not correlative to fibre responses. The latter implies that an increase in fibre response is due to an increase in the total mass in the gaseous sample rather than an increase in air velocity. This could likely be due to the fact that in all cases, air velocities are higher than a certain critical value (by some authors defined to be  $10 \text{ cm s}^{-1}$  as stated in the introduction) and therefore it does not have an additional impact on the thickness of the boundary layer.

Finally, a test on the influence of Reynolds numbers on sampling has been performed since the different points were obtained with completely different designs and different values of Reynolds numbers (flow regime). In consequence, evidence is given on the fact that this is not either a crucial parameter affecting sampling efficiency.

The results presented here are providing a useful approach to calibrate the methodology of SPME with adsorptive fibres simply based on the total mass of compounds in the gaseous sample and it is applicable to a wide range of air velocities, flow rates and Reynolds numbers. It represents in consequence a very practical approach that makes it possible to calibrate without applying complex theoretical models.

#### 4. Summary and conclusions

In the EUPHORE chambers, we have already successfully applied [20,21] the methodology of SPME for the determination of gaseous carbonyls. In addition, we have carried out studies to characterise the occurrence of certain undesirable effects that can hinder the quantity of the methodology [22]. This work is a continuation of our efforts to increase the knowledge on SPME methodology by developing a system of active sampling based on fluid dynamics that could be applied to field sampling studies. This form of sampling was initially developed to sample directly from the chambers [23]. In this work we intended to make it transferable to any other gaseous system. The effect of experimental parameters such as flow rate, Reynolds numbers, air velocity and total mass of analyte on the quantity of the methodology and reproducibility has been investigated in the present study.

The work carried out comprises the preliminary characterisation work required for automation of the methodology. Automation is important to make the methodology more robust by decreasing the variability introduced by manual sampling. Manual sampling is cumbersome and prone to important variability.

These efforts have been made to attain the versatility and sensitivity required in product studies on atmospheric reactions, which proceed quickly since depletion of the products formed in the reactions occurs rapidly through photo-degradation with oxidants [24,25]. This would allow reducing the sampling times in order to improve sampling acquisition during the experiments, essential to obtain reaction profiles.

Hence, contrary to the generally accepted idea that Solid Phase Microextraction can only be used from a qualitative prospective, we have demonstrated that in fact quantitation is possible.

#### Appendix A. Supplementary data

Supplementary data associated with this article can be found, in the online version, at doi:10.1016/j.talanta.2011.10.039.

#### References

- [1] G. Ouyang, J. Pawliszyn, *Trends Anal. Chem.* 25 (7) (2006) 692–703.
- [2] J.A. Koziel, M. Jia, J. Pawliszyn, *Anal. Chem.* 72 (2000) 5178–5186.
- [3] Y. Chen, J.A. Koziel, J. Pawliszyn, *Anal. Chem.* 75 (2003) 6485–6493.
- [4] K. Sukola, J.A. Koziel, F. Augusto, J. Pawliszyn, *Anal. Chem.* 73 (1) (2001) 13–18.
- [5] R.J. Bartelt, B.W. Zilkowski, *Anal. Chem.* 72 (16) (2000) 3949–3955.
- [6] G. Ouyang, J. Cai, X. Zhang, H. Li, J. Pawliszyn, *J. Sep. Sci.* 31 (6–7) (2008) 1167–1172.
- [7] S.N. Zhou, X. Zhang, G. Ouyang, A. Es-haghi, J. Pawliszyn, *Anal. Chem.* 79 (2007) 1221–1230.
- [8] F. Augusto, J.A. Koziel, J. Pawliszyn, *Anal. Chem.* 73 (3) (2001) 481–486.
- [9] Q. Wang, J. O'Reilly, J. Pawliszyn, *J. Chromatogr. A* 1071 (1–2) (2005) 147–154.
- [10] P.A. Martos, J. Pawliszyn, *Anal. Chem.* 69 (1997) 206–215.
- [11] C.V. King, *J. Am. Chem. Soc.* 57 (1935) 828–831.
- [12] R. Darby, *Chemical Engineering Fluid Mechanics*, second ed., Marcel Dekker, New York, 2001.
- [13] E. Costa, *Ingeniería Química*, vol. 3, Flujo de fluidos, Alhambra, 1985.
- [14] J.M. Coulson, J.F. Richardson, *Chemical Engineering, Volume 1: Fluid Flow, Heat Transfer and Mass Transfer*, sixth ed., Butterworth-Heinemann, 1999.
- [15] F.A. Holland, R. Bragg, *Fluid Flow for Chemical Engineers*, second ed., Edward Arnold, London, 1995.
- [16] O. Levenspiel, *Chemical Reaction Engineering*, third ed., Wiley, New York, 1993.
- [17] M.C. Potter, D.C. Wiggert, *Mechanics of Fluids*, third ed., Thomson Learning, Pacific Grove, CA, USA, 2002.
- [18] B.J. Finlayson-Pitts, J.N. Pitts Jr., *Chemistry of the Upper and Lower Atmosphere*, Academic Press, San Diego, CA, 2000.
- [19] E.C. Apel, T. Brauers, R. Koppmann, R. Tillmann, C. Holzke, R. Wegener, J. Boßmeyer, A. Brunner, T. Ruuskanen, M. Jocher, C. Spirig, R. Steinbrecher, R. Meier, D. Steigner, E. Gómez Alvarez, K. Müller, S.J. Solomon, G. Schade, D. Young, P. Simmonds, J.R. Hopkins, A.C. Lewis, G. Legreid, A. Wisthaler, A. Hansel, R. Blake, K. Wyche, A. Ellis, P.S. Monks, *J. Geophys. Res.* 113 (2008) D20307, doi:10.1029/2008JD009865.
- [20] E. Gómez Alvarez, E. Borrás, J. Viidanoja, J. Hjorth, *Atmos. Environ.* 43 (2009) 1603–1612.
- [21] E. Gómez Alvarez, J. Viidanoja, A. Muñoz, K. Wirtz, J. Hjorth, *Environ. Sci. Technol.* 41 (2007) 8362–8369.
- [22] E. Gómez Alvarez, M. Valcárcel, *Talanta* 77 (2009) 1444–1453.
- [23] E. Gómez Alvarez, *Talanta* 72 (2007) 1757–1766.
- [24] S. Net, E. Gómez Alvarez, S. Gligorovski, H. Wortham, *Atmos. Env.* 45 (2011) 3007–3014.
- [25] S. Net, E. Gomez Alvarez, N. Balzer, H. Wortham, C. Zetzsch, S. Gligorovski, *ChemPhysChem.* (2010) 4019–4027.